Neutron Induced Radiography. A Technique to Inspect the Internal Structure of thin Samples

M. A. Stanojev Pereira, F. Pugliesi, and R. Pugliesi *
Instituto de Pesquisas Energéticas e Nucleares (IPEN-CNEN/SP)
Av. Prof. Lineu Prestes 2242, Cidade Universitária, Butantã
CEP 05508-000, São Paulo-SP, Brazil
(Received on 3 July, 2008)

The present paper describes a radiography technique to inspect low thickness samples, on the order of micra. The penetrating radiation are charged particles generated by a lithium fluoride screen irradiated by thermal neutrons. The film used to register the images is a solid state nuclear track detector and the experimental conditions to obtain the best radiography are provided. A digital system for data acquisition and image processing was also used.

Keywords: Track detectors; Track - etch foils; Radiography

1. INTRODUCTION

There is a great scientific interest regarding the inspection of the internal structure of thin samples, on the order of micra, in biology, medicine, forensic technology, metallurgy, etc. Radiography and microscopy techniques are commonly used for such purpose. Among these techniques, the autoradiography which records the distribution and location of a radioactive liquid material within the sample, is one of the most used [1, 2, 3, 4].

The present paper describes a radiography technique to inspect thin samples in which charged particles, generated by a lithium fluoride screen irradiated by thermal neutrons, are used as penetrating radiation. The film used to record the image is a solid state nuclear track detector – SSNTD. In this case the interaction of the charged particles with the detector gives rise to damages in its molecular structure which under an adequate chemical etching became tracks, the basic units that form the image [5].

A digital system developed by the neutron radiography working group of IPEN-CNEN/SP was used for data acquisition and image processing [6].

The main objective of this paper is to determine the exposure and the etching time for which the set detector – screen must be submitted to obtain the best contrast in the radiographic image, evaluate the spatial resolution for these conditions and provide some radiography images to show the technique's capability.

2. EXPERIMENTAL

The irradiations have been performed at the neutron radiography facility installed at radial beam hole #8 of the 5MW pool - type IEA-R1 nuclear research reactor of IPEN – CNEN/SP. The thermal neutron flux near the reactor core is about $\sim 10^{13}$ n. $s^{-1}cm^{-2}$ and the characteristics of the neutron beam at the detector irradiation position are given in Table I [7].

TABLE I: Characteristics of the neutron beam at the detector position.

Flux at the irradiation position	1.75×10^6 n/cm^2.s
Beam diameter	20cm
Mean energy	7meV

The SSNTD used was the CR-39 which is a polymer manufactured by Pershore Mouldings England, having 600μm in thickness. The lithium fluoride screen (LiF) is a neutron scintillator commercially known as NE-426. In its manufacturing process a mixture of ^{6}LiF and ZnS is deposited on a 18cm x 24cm aluminum base. The interaction "neutron – screen" gives rise to the nuclear reaction ^{6}Li(n,α)T generating the charged particles with energies of 2.05 MeV and 2.74 MeV respectively [8].

During irradiation, the CR-39, the sample and the LiF screen are kept, in this order with respect to the neutron beam, in a tight contact inside an aluminum cassette as shown in Fig. 1. The neutrons pass through the detector, through the sample and will induce nuclear reactions in the screen. The generated particles reach the sample and the transmitted intensity impinges the SSNTD. The interaction of these particles with the detector leaves a narrow and permanent trail of damages with diameters of about 100 Angstroms and length of about 54μm and 10μm, the range of the tritium and of the α - particles in the SSNTD [9]. Under an adequate chemical etching the damaged regions being more reactive than the surrounding undamaged areas are enlarged forming permanent tracks, the responsible by the darkening of the detector and therefore by the image formation [10].

The etching was performed in a KOH (30%) aqueous solution at 70 $^\circ$C [11]. During the etching, the CR-39 remains inserted in a Pyrex container, containing 400 ml of the solution and this set is immersed in a heated water bath. After etching, the detector is washed in a soft water stream.

In order to determine the conditions to obtain the best contrast in the image, the parameter "light transmitted intensity" through the irradiated and etched CR-39 detectors must be evaluated. This was performed in the digital system by using a transmission scanner coupled to a computer and a software. The darkening of the detector was quantified in a 8 bits gray

*Corresponding author: e-mail: pugliesi@ipen.br

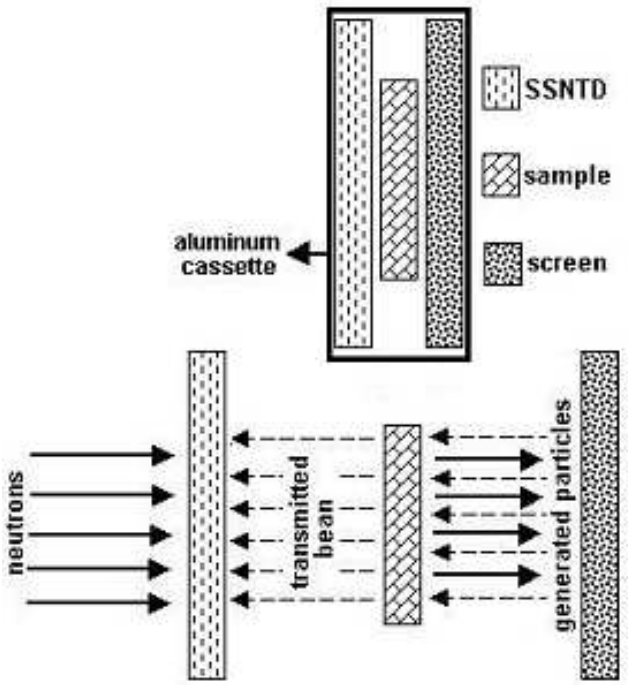

FIG. 1: Set up of the neutron induced radiography experiment where the neutron beam is converted into alpha and tritons, detected by a SSNTD.

level scale ranging from 0 (darkest pixel) to 255 (brightest pixel) [6].

3. DATA ACQUISITION AND ANALYSIS

3.1. Contrast

Usually the contrast in a SSNTD is studied by means of curves that relate gray level intensity (GL) and exposure (E) as a function of the etching time and is defined by the equation [6]:

$$G = \frac{\Delta(GL)}{\Delta log(E)} \quad (1)$$

Hence the best contrast is obtained for the exposure interval corresponding to the steeper region of these curves. Since the charged particles are generated by neutrons, these curves were obtained as functions of the neutron exposure given by:

$$E = \phi \cdot t \quad (2)$$

where ϕ is the neutron flux at the detector(n.s^{-1}.cm^{-2}) and t is the irradiation time (s).

For such purpose several slices of the detector (15mm x 35mm) have been irradiated in the exposure interval 1.75x10^{7}n.cm^{-2} < E < 1.89x10^{10}n.cm^{-2} and etched in 15, 35 and 65 minutes. These etching times were selected by taking into account some previous results obtained in [12]. The detectors have been positioned in the scanner and the behavior of the gray level as functions of the exposure for these etching times is shown in Fig. 2. Each experimental data was obtained by averaging the gray level values of about 15,000 individual pixels in an area of 0.4cm^2 of the detector. According to the obtained results the best contrast was achieved for 35 minutes of etching and for the exposure interval 1x10^9 < E < 1.5x10^{10}n.cm^{-2} (indicated by arrows). This means that the required exposure to reach the best contrast, that is, for which the detector reaches the highest darkening level is 1.5x10^{10}n.cm^{-2} and according to (2) and to Table I, corresponds to an irradiation of 2.4 hours. For 15 minutes of etching, the value for the contrast and for the dynamic range (the gray level range corresponding to the best contrast region) are very near to the obtained for 35 minutes, however an irradiation of about 11 hours is necessary to reach the best contrast region. For 65 minutes the irradiation time is only 1 hour, however the contrast and the dynamic range are worst when compared with the previous values. These results are summarized in Table II.

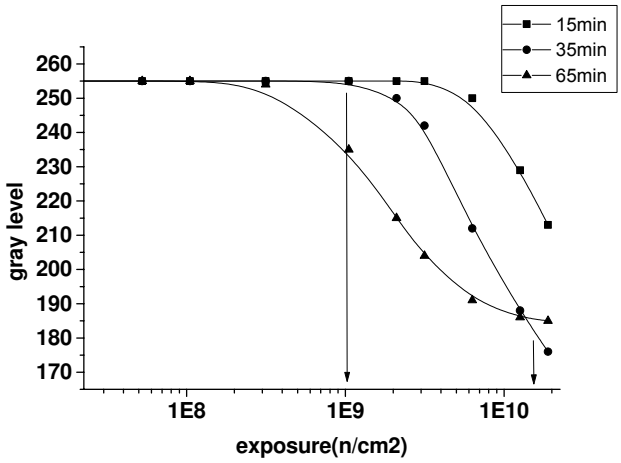

FIG. 2: Behavior of the gray level as functions of the exposure for 15, 35 e 65 minutes of etching.

TABLE II: Contrast characteristics for the CR-39/ LiF.

Etching time (min)	Contrast	Irradiation time (h)	Dynamic range
15	62	11	75
35	68	2.4	80
65	55	1	58

3.2. Spatial Resolution

The spatial resolution is defined as the capability of making distinguishable the individual parts of an object closely adja-

cent. The resolution depends of the thickness of the sample, sample to detector distance, track size, range of the particles in the SSNTD and neutron beam and screen inhomogeneities [13, 14]. Usually the resolution is quoted in terms of the parameter "total unsharpness - (Ut)" which is evaluated by scanning the gray level intensity at the radiography image of a sharp edge object, obtained at the same conditions for which the best contrast was determined, that is, 35 minutes of etching and 2.4 hours of irradiation. In the present paper the sharp edge object was a cellulose nitrate foil 100μm in thickness. After irradiation and etching the detector was positioned in the digital system and the scanning performed at 3200 d.p.i (dots per inch). The Fig. 3 shows a typical obtained gray level distribution. The following Edge Spread Function-ESF was fitted to the distribution intensity:

$$ESF = p1 + p2.\arctan(p3.(X - p4)) \qquad (3)$$

where X is the scanning coordinate, $p1$, $p2$, $p3$ e $p4$, are free parameters and the total unsharpness is given by $Ut = 2/(p3)$ [15].

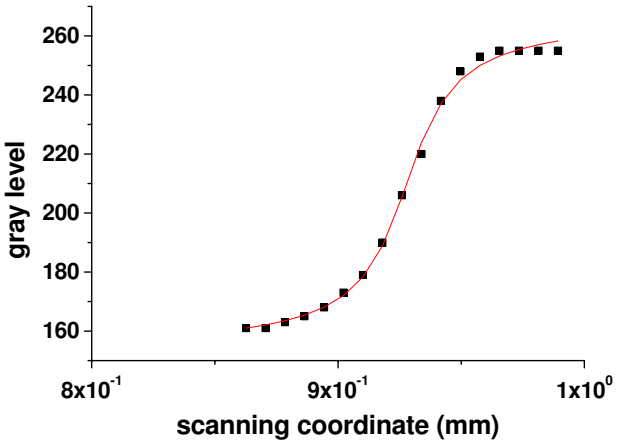

FIG. 3: Typical gray level intensity distribution and the ESF fitting.

The obtained result was Ut = 47±2 μm which has been determined by averaging the unsharpness values corresponding to four distinct regions of the edge and its uncertainty is given by the standard deviation of the mean. The results are given in Table III. This result is in accordance to the image formation theory in SSNTD and a detailed analysis can be found in [10, 12, 13].

TABLE III: Total unsharpness: four distinct regions of the edge and its mean value.

Measurement	Ut(μm)
1	43±5
2	49±5
3	50±6
4	46±5
Mean value	47±2

4. CONCLUSION

The Table IV summarizes the irradiation and etching conditions to obtain the best contrast in the radiography as well as the characteristics of the image for the CR-39 – LiF set.

TABLE IV: Conditions and characteristics of a radiography.

Exposure interval (n.cm^{-2})	$1\times10^9 < E < 1.5\times10^{10}$
Irradiation time (h)	2.4
Etching time (min)	35
Contrast	68
Dynamic range	80
Spatial resolution (μm)	47±2
Maximal sample thickness (μm)	$\sim$ 54

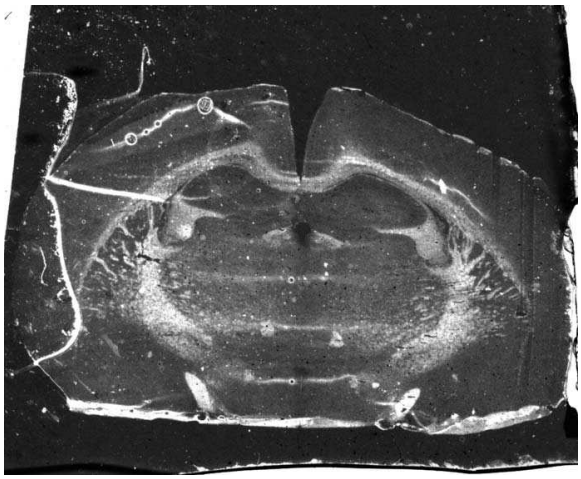

FIG. 4: Mice brain tissue - 10μm in thickness.

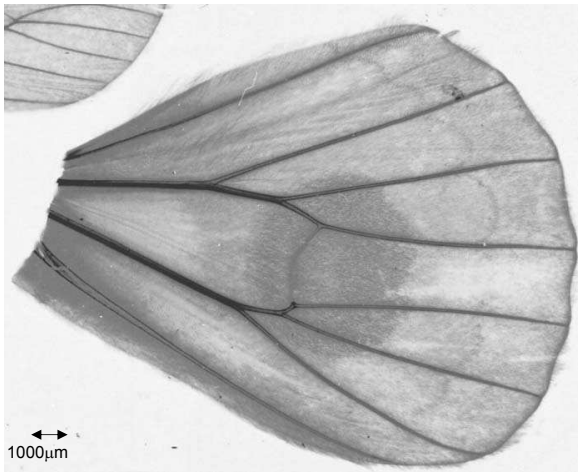

FIG. 5: Insect wing showing the nutrients within the ducts (viens).

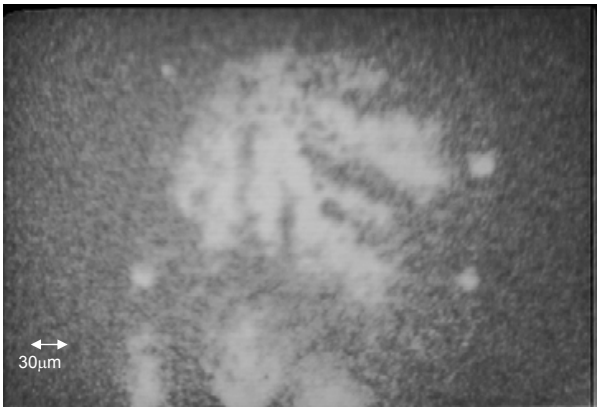

FIG. 6: Bacterial colony.

In order to demonstrate the potential of this technique, the figures below are some radiographs, obtained in the conditions given in Table IV. In these examples, the radiographs have been digitized at 3200 d.p.i and its visualization has been enhanced by digital processing by using the same digital system. The Fig. 4 shows the radiography of a mice brain tissue having 10 μm in thickness. The sample was cut and deposited at the CR-39 surface and covered by the LiF screen. After irradiation and etching the CR-39 is positioned in the digital system and the resulting image shows many details of the tissue structure. The Fig. 5 shows the radiography of an insect wing obtained as the previous one. It is possible to observe details of its internal structure as the ducts (or viens) for the nutrients with diameter ranging from 60μm to 200μm. In the Fig.6 a radiography of bacterial colony is shown. In this case the radiography was obtained by taking an aliquot of the cultured medium in which the colony was growing and depositing it on the CR-39 surface. After its drying, it was covered by the screen and the detector was irradiated and etched. The resulting image shows several details of a selected colony.

In comparison with the autoradiography, in the present technique is not necessary to handle a radioactive liquid material to perform the radiography, the irradiation time to obtain the radiography is some hours instead of weeks or months and the image quality is better [16].

It is important to mention that other screen can be used to generate other penetrating radiations. For example two commercially available screens manufactured by Kodak, based on natural boron or lithium tetraborate, have been already studied and their characteristics are detailed in [17]. In the same way other detectors can be also used to register the radiography image, and detailed studies regarding the Makrofol-E, Makrofol-DE and Durolon are published in [18].

[] G. Waksman, E. Hamel, M. Fournie-Zaluski, and B. P. Roques, Proc. Natl. Acad. Sci. **83**, 1523 (1986).

[] M. P. Ginige, P. Hugenholtz, H. Daims, M. Wagner, J. Keller, and L. L. Blackall, Applied and Environmental Microbiology **70,** No.1 588 (2004).

[] A. S. Mghir, A. C. Cremieux, R. Bleton, F. Ismael, M. Manteau, S. Dautrey, L. Massias, L. Garry, N. Sales, B. Maziere, and C. Carbon. Antimicrobial Agents and Chemotherapy **42,** No. 11 2830 (1998).

[] I. Cloez-Tayarani, A. Cardonia, J. Rouselle, O. Massot, L. Edelman, and G. Fillion, Proc. Natl. Acad. Sci.**94**, 9899 (1997).

[] M. Lferde, Z. Lferde, M. Monnin et al, Nucl. Tracks Radiat. Meas. **8,** 497 (1984)

[] F. Pugliesi, V. Sciani, M. A. Stanojev Pereira, and R. Pugliesi, Braz. J. Phys. **37,** no. 2A, 446 (2007).

[] R. Pugliesi, M. A. Stanojev Pereira, M. A. P. V. de Moraes, and M. O. de Menezes, International Journal of Applied Radiations and Isotopes. **50,** 375 (1997).

[] M. R. Hawkesworth, Atom. Energy Rev. **152**, 169 (1977).

[] http://physics.nist.gov/PhysRefData/Star/Text/ASTAR.html

[] R. Ilic' and M. Najzer, Nucl. Track Radiat. Meas. **17**, 453 (1990a).

[] S. A. Durrani, R. K. Bull, Solid State Nuclear Track Detection. Principles, Methods and Applications. International Series in Natural Philosophy vol-111, Pergamon Press(1987).

[] M. A. Stanojev Pereira, PhD Thesis, IPEN-CNEN/SP (2008).

[] R. Ilic' and M. Najzer, Nucl. Track Radiat. Meas. **17**, 461 (1990b).

[] R. Pugliesi, M. A. Stanojev Pereira, Nuc Instruments and Methods in Physics Research(A), **484**, 613 (2002).

[] A. A. Harms and A. A. Zellinger, Phys. Med. Biol. **22**, n ° 1 70 (1977).

[] L. F. Belanger and C. J. Belanger, Biophysic. and Biochem. Cytol. **6**, No. 2, 197 (1959).

[] M. A. Stanojev Pereira, R. Pugliesi, and F. Pugliesi, Radiations Measurements. Accepted for publication in Feb/2008.

[] F. Pugliesi, PhD Thesis. IPEN-CNEN/SP (2008).